Small-x saturation in forward hadronic interactions

Hirotsugu Fujii[1,*]

[1]Institute of Physics, University of Tokyo, Komaba, Tokyo 153-8902, Japan

Abstract. After a brief introduction of parton saturation in hadrons at small Bjorken's x, we recapitulate its phenomenological implications in high-energy particle production, such as longitudinal correlation, particle mulctiplicity, limiting fragmentation and charm quark production, which may have relevance to study of high-energy cosmic ray physics.

1 Introduction

In high-energy hadron scatterings, copious particles are produced over a wide range of rapidity interval $Y^{\rm tot} = 2\ln\sqrt{s}/m$ with $\sqrt{s}$ being the collision energy and m the incident hadron mass. The scattered partons have only small momentum fractions $x_{1,2}$ of their parent hadrons, and the rapidity interval between the projectile hadron and the scattered parton is filled with numbers of gluons radiated successively with a probability of order $\alpha_s \ln(1/x_{1,2}) \sim$ O(1): A hadron in very high-energy collisions is regarded as a dense gluonic system.

In terms of transverse momentum p_T and rapidity y of the produced particle, the momentum fractions carried by the partons are expressed as $x_{1,2} = (p_T/\sqrt{s})e^{\pm y}$ in 2→1 kinematics. In the forward rapidity region, $x_1 \gg x_2$, or *vice versa*, one of the momentum fractions becomes extremely small. At the LHC energy $\sqrt{s} = 14$ TeV, the rapidity interval becomes $Y^{\rm tot} \sim 19$ and $x_2 \sim 10^{-6}$ at $p_T = 2$ GeV/c and $y = 4$. In cosmic-ray events of (e.g.) $\sqrt{s} \sim 100$ TeV, we have $Y^{\rm tot} \sim 23$ and can probe even much smaller x_2 which is out of reach in laboratory experiments.

Dense gluonic state observed in high-energy hadron scatterings will reveal a universal aspect of QCD, parton saturation, which is characterized by an emergent dynamical scale Q_s, called saturation momentum [1–3]. In the next section we briefly recapiturate the parton saturation at small x, and its effective description in QCD, and then discuss some of its implications in the following sections.

2 High-energy hadron scattering and saturation

2.1 Parton saturation

Small-x gluons are short-time fluctuations in the wave function of a composite hadron. The higher the energy is, the longer becomes the lifetime of these gluons by Lorentz time dilation. Then as colored particles these gluons radiate additional gluons and the system becomes denser.

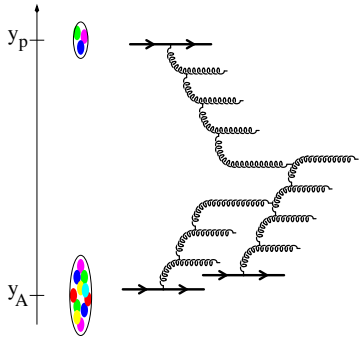

Figure 1. Schematic picture of a high-energy pA collision. The gluons emitted from the color sources split to two gluons successively in rapidity space, and they can merge together when the system becomes dense, before the gluon production.

When the gluon density $xg(x, Q_s)$ multiplied with the interaction area "α_s/Q_s^2" reaches to a value comparable to the hadron size πR_h^2, the gluon merging process starts to balance against the gluon splitting, wihch determines the saturation scale $Q_s^2(x)$. As a result of this non-linear effect, the system is in the gluon saturation regime at the resolution scale (transferred momentum) Q^2 less than $Q_s^2(x)$. The phase space density of the gluons is then estimated as $dN/d^2r_T d^2p_T \sim 1/\alpha_s$.

Note that, although small-x gluons themselves are very short-time fluctuations, the color sources which emit these gluons are pre-formed in the non-linear evolution long before the instant of the collision. In other words, small-x gluons bear the effects of color fluctuations added up coherently over the hadron size. Note also that the saturation scale for a heavy nucleus $Q_{s,A}^2$ is enhanced from that of the proton $Q_{s,p}^2$ by a factor of the nuclear thickness $A^{1/3}$ as $Q_{s,A}^2 \sim A^{1/3}Q_{s,p}^2$ with A being the nuclear mass number.

2.2 Color Glass Condensate effective theory

The Color Glass Condensate (CGC) effective theory is based on an arbitrary separation of the gluon degrees of

*e-mail: hfujii@phys.c.u-tokyo.ac.jp

freedom into small- and large-x parts in the wave function, and it provides a framework for describing the evolution of the color source functional $W_y[\rho]$ taking account of the gluon splitting and merging processes with increasing rapidity $y = \ln(1/x)$. When $Q_s(x) \gg \Lambda_{\rm QCD}$ and $\alpha_s(Q_s) \ll 1$, small-coupling techniques may be applied even in the dense regime of the hadron wave function. We can deal with this dense gluon system nonperturbatively by solving the evolution equation for $W_y[\rho]$ with the kernel evaluated at the small coupling in the CGC effective theory.

As the effective degree of freedom in high-energy scatterings, we take an eikonal amplitude of a color dipole traversing the target,

$$\mathcal{N}(\boldsymbol{x}_T, \boldsymbol{y}_T, y) = \int [D\rho]\, W_y[\rho] \left[1 - \frac{1}{N_c}\mathrm{tr}(U(\boldsymbol{x}_T)U^\dagger(\boldsymbol{y}_T))\right], \tag{1}$$

where $\boldsymbol{x}$ and $\boldsymbol{y}$ are the transverse positions of the probe charges in fundamental representation and $U(\boldsymbol{x})$ is the eikonal phase factor acquired by each probe charge. The amplitude is averaged over the color source functional $W_y[\rho]$ in the target. In the large N_c limit, the fundamental and adjoint dipole amplitudes are simply related as

$$1 - \mathcal{N}_A = (1 - \mathcal{N})^2\,. \tag{2}$$

The dipole amplitude in the adjoint representation is related to the unintegrated gluon distribution (UGD) function $\varphi(\boldsymbol{k}, x; \boldsymbol{b})$ via the Fourier transformation w.r.t. $\boldsymbol{x} - \boldsymbol{y}$:

$$\varphi(\boldsymbol{k}, x; \boldsymbol{b}) = \frac{C_F}{\alpha_s(k)(2\pi)^3}\mathrm{F.T.}\nabla^2\mathcal{N}_A(\boldsymbol{x}, \boldsymbol{y}, y), \tag{3}$$

where $\boldsymbol{b} = (\boldsymbol{x} + \boldsymbol{y})/2$ is the center-of-mass position of the dipole. One should note that this $\varphi(\boldsymbol{k}, x; \boldsymbol{b})$ includes higher-oder twist effects and in this sense it is a generalization of the UGD function defined at the leading-twist level.

As we noticed that the gluon distribution evolves as we change the relevant value of x by boosting the hadron. This x dependence for the dipole amplitude is concisely described by the Balitsky-Kovchegov (BK) evolution equation (in the large N_c limit) as

$$\frac{\partial\mathcal{N}(r,y)}{\partial y} = \int d^2\boldsymbol{r}_1\; K^{\rm run}(\boldsymbol{r}_1, \boldsymbol{r}; \alpha_s)\,[\mathcal{N}(r_1, y) + \mathcal{N}(r_2, y) - \mathcal{N}(r, y) - \mathcal{N}(r_1, y)\mathcal{N}(r_2, y)], \tag{4}$$

where $\boldsymbol{r}_{1,2}$ and $\boldsymbol{r}$ with $\boldsymbol{r}_2 = \boldsymbol{r} - \boldsymbol{r}_1$ are the transverse sizes of the dipoles, and $K^{\rm run}$ is the evolution kernel with the running coupling corrections in Balitsky's prescription. We abbreviate this as rcBK equation. This equation resums the gluon radiation corrections of order $(\alpha_s \ln 1/x)^n$ in the dilute regime. The non-linear term restores local unitality in the dense regime; without it the amplitude $\mathcal{N}$ would blow up. Here we have ignored the impact parameter dependence of $\mathcal{N}$.

The dipole amplitude for the nucleon is constrained by global analysis of lepton-proton scattering data at $x < 0.01$[4]. For example, we show in Fig. 2 the dipole amplitude $\mathcal{N}_A(k, y)$ obtained by the global analysis using the rcBK evolution for $x < 0.01$ with the MV$^\gamma$-model initial condition set at $x_0 = 0.01$ [4, 5]. The saturation scale $Q_s(x)$ can be defined as the peak position of the amplitude $k^2 N_A(k, y)$. We see that it moves toward the larger values under the rcBK evolution because gluon splitting increases the number of the gluons at larger k_T and gluon merging decreases it at smaller k_T.

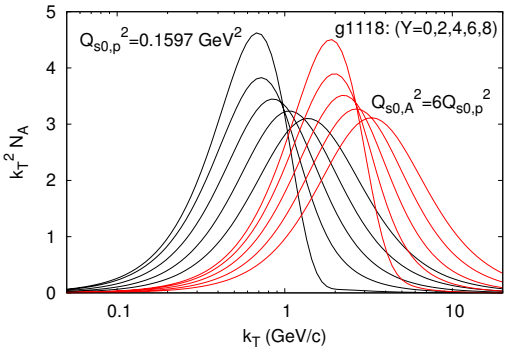

Figure 2. The x-evolution of the Fourier transform of the dipole amplitude $\mathcal{N}_A(k, Y)$. The initial saturation scale at $x_0 = 0.01$ is set to $Q_{s0,p}^2 = 0.1597$ GeV^2 for the proton and $Q_{s0,A}^2 = Q_{s0,A}^2$ for a heavy nucleus. The rapidity is defined by $Y = \ln x_0/x$ with $x_0 = 0.01$.

Global analysis of high-energy lepton-*nucleus* scattering data is not available yet, and we need to rely on modeling of the dipole amplitude for a nuclear target. In an approach, we multiply a factor of $A^{1/3}$ to the initial saturation scale at $x_0 = 0.01$, taking account of the average target thickness. In another approach, we distribute the nucleons in the nuclear target with a probability proportional to the Woods-Saxon nuclear profile and determine the initial saturation scale $Q_{s0,A}^2(\boldsymbol{b})$ locally in the transverse position $\boldsymbol{b}$ by counting the number of the nucleons on the straight-line trajectory of the probe parton. This latter treatment of the target is called the Monte Carlo (MC) Glauber model.

In Fig. 2, for comparison, we also show the dipole amplitude obtained by the rcBK equation as in the proton case but with the initial saturation scale multiplied by a factor of $A^{1/3} = 6$, i.e., $Q_{s0,A}^2 = 6Q_{s0,p}^2$. The amplitude $k^2\mathcal{N}_A$ of the nucear target is now peaked at the larger value of k_T than in the proton case, reflecting the enhancement of the gluon density per unit area by the nucleus thickness factor. We expect that gluon saturation will give more distinctive effects on heavy nucleus collisions even at moderately small x values.

In this presentation we show the numerical results with the CGC framework valid at the leading-order (LO) accuracy. Although next-to-leading-order (NLO) extension of the framework has been recently intensively investigated [6–8], its phenomenological applications are still not available yet.

3 Phenomenology

Now we discuss some selected topics of the parton saturation in the small-x regime probed by high-energy hadron interactions.

3.1 Initial stage of heavy ion collisions

High-energy heavy-ion collision experiments have been performed at RHIC and the LHC, to create a dense medium of quarks and gluons and to study its collective properties. Although the main concern of these studies is collective behavior of the created medium, the initial-stage dynamics is certainly important as well for completing our understanding of the evolution of nucleus collisions and extracting the effects of the late-time dynamics from the observable data.

In high-energy hadron collisions, we regard the nucleus as the fluctuating color charges traveling almost at the speed of light and frozen during the initial impact. This situation can be formulated as a collision of the two strong color sources on the light-cone, each of whose densities is inversely proportional to the coupling constant, α_s. The leading-order solution is provided by solving the classical equation of motion of the fields. And then we average the solutions over the fluctuation distribution $W_y[\rho]$. The small-x gluon density per transverse area is enhanced by a nuclear thickness factor of $A^{1/3}$ for a heavy nucleus, which makes the classical approximation more suitable there.

The initial classical field strengths are Lorentz contracted and localized like thin sheets around the projectile and the target nucleus, i.e., the Weizsäcker-Williams fields. The single dimensionful parameter Q_s characterizes the field strength and the correlation length of the color fields in the transverse directions. This CGC framework has been successfully applied for describing the energy dependence as well as the impact-parameter dependence of the particle multiplicity in heavy-ion collision experiments [3].

It has been noticed that, during passing through each other, the initial classical color fields with transverse polarization turn to longitudinally polarized electric and magnetic fields via the non-Abelian interactions. This field configuration provides a typical initial condition for subsequent time-evolution of the heavy-ion collisions in the CGC picture.

Meanwhile, one of the most intriguing findings in experiments is the long-range rapidity correlation, so-called "ridge" structure, observed in two-particle distributions in nucleus-nucleus collisions at RHIC, and later found even in proton-proton (p-p) and proton-nucleus (p-A) collisions at the LHC. The long-range rapidity correlation must be imprinted in a very early stage of the event as required by causality. The longitudinal color field configuration as a particle source is expected to be in the origin of the rapidity correlation [9], and model studies are underway.

The initial configuration of longitudinal color electric and magnetic fields also offers a unique opportunity for studying the topological charge fluctuations and anomaly of QCD, through chiral magnetic effect, in laboratory experiments.

3.2 Particle multiplicity in dilute-dense collisions

In forward particle production in hadron collisions, where $x_1 \gg x_2$, we probe the dense partons, mostly the gluons, of the target B with the dilute partons of the projectile A. It is known that, for a collision of such a dilute-dense system where $Q_s(A) \sim \Lambda_{\rm QCD} \ll Q_s(B)$, one can derive the gluon production formula in the k_T-factorized form at leading order in α_s but including all order contributions from the dense target via the UGD function $\varphi(\boldsymbol{k}_T, y)$ [10]:

$$\frac{d\sigma^{A+B\to g}}{dy\, d^2p_T\, d^2R} = K^k \frac{2}{C_F}\frac{1}{p_T^2}\int^{p_T}\frac{d^2k_T}{4}\int d^2b\;\alpha_s(Q) \times \varphi_P\left(k_1, x_1; b\right)\;\varphi_T\left(k_2, x_2; R-b\right)\,, \quad (5)$$

where $\boldsymbol{k}_{1,2} = (\boldsymbol{p}_T \pm \boldsymbol{k}_T)/2$, and $C_F = (N_c^2-1)/2N_c$. We have deteremined the initial saturation scales locally at the positions, $\boldsymbol{b}$ and $\boldsymbol{R}-\boldsymbol{b}$, respectively, for the dilute projectile and dense target. The scale of the running coupling is chosen here to $Q = \max(k_1, k_2)$. Most importantly, the x-dependence of $\mathcal{N}_A$ obtained by solving the rcBK equation encodes all the collision energy and rapidity dependence of the gluon production formula (5). The normalization factor K^k lumps together higher-order corrections, sea-quark contributions and other dynamical effects not included in the CGC formulation.

When x_1 exceeds $x_0 = 0.01$, the so-called hybrid formalism is expected to be better suited for particle production, which at leading order in α_s reads

$$\frac{dN_h}{dy\, d^2p_T} = \frac{K^h}{(2\pi)^2}\int_{x_F}^1\frac{dz}{z^2}\Big[x_1 g(x_1, Q^2)\mathcal{N}_A\left(x_2, k_T\right) D_{h/g}(z, Q^2) + (\text{quark contrib.})\Big]\,, \quad (6)$$

where the gluons from the projectile are described by collinear parton distribution function (PDF) $g(x, Q^2)$, and the small-x gluons in the dense target are expressed by the UGD function $\sim k_T^2\mathcal{N}_A(x, k_T)$ with $k_T = p_T/z$. Contributions from the process initiated by the quarks from the projectile are also included in the calculations, though not written explicitly. Use of UGD takes care of the effects of x-evolution as well as the multiple scatterings of the projectile parton in the target. The hadronization of the scattered parton into a hadron h is described by the usual fragmentation function (FF), $D_{h/j}$. Both PDF and FF are evaluated at the factorization scale Q, which we set within the range of $Q = (p_T/2, 2p_T)$.

We found in Ref. [5] that p_T dependence of the single particle distribution in proton-(anti)proton collisions at $\sqrt{s} = 1.96$ and 7 TeV is well described with the UGD function $k_T^2\mathcal{N}_A(x, k_T)$ after K^h is fixed to fit the data at $p_T = 1$ GeV. This provides a consistency check for the use of the UGD function which is constrained by DIS global analysis, because the p_T spectrum reflects the x dependence of the UGD in eq. (6).

The p_T-integrated hadron multiplicity is crudely estimated on average from that of the initially produced gluons (5) by assuming a proportionality relation between the two with a constant κ_g. The energy dependence of the multiplicity obtained by eq. (5) was found consistent with the

data of p-p collisions at $\sqrt{s} = 2.76$ and 7 TeV. The parameter set was used to estimate the charged hadron multiplicity in p-Pb collisions at $\sqrt{s} = 5.02$ TeV at mid-rapidity successfully in Ref. [5]. The rapidity distribution was steeper than the data, but one should note that a Jacobian with typical hadron mass was used to convert the rapidity to the pseudo-rapidity there.

Next let us discuss the so-called nuclear modification factor $R_{\mathrm{p}+A}(p_T)$ of the single inclusive charged hadrons, which is defined as

$$R_{\mathrm{p}+A}(p_T) = \frac{1}{\langle N_{\mathrm{coll}} \rangle} \frac{dN_{\mathrm{ch}}^{\mathrm{p}+A}/d\eta d^2p_T}{dN_{\mathrm{ch}}^{\mathrm{p}+\mathrm{p}}/d\eta d^2p_T} \tag{7}$$

with $\langle N_{\mathrm{coll}} \rangle$ being the average number of nucleon-nucleon collisions in a proton-nucleus event. This quantity is unity if the event is a simple superposition of nucleon-nucleon collisions, and its deviation indicates the existence of the nuclear effects. The stronger parton saturation in a heavier target generally leads to a suppression of $R_{\mathrm{p}+A}$ at $p_T \lesssim Q_s(x)$.

In Fig. 3, we show $R_{\mathrm{p}+A}(p_T)$ of the charged hadrons in p-Pb collisions at the collision energy $\sqrt{s} = 5$ TeV. In the top panel is shown the result at the mid-rapidity $\eta = 0$, where both the gluons from the projectile and the target have small x values and we use k_T-factorized formula (5). In this case the ratio is suppressed at $p_T \lesssim 2$ GeV/c, which is expected from the gluon saturation at small x. At higher $p_T \gtrsim 2$ GeV/c, on the other hand, it increases and even becomes slightly higher than unity , though it has a large uncertainty (gray band). Our prediction is found to be consistent with experimental data at the LHC [11]. The result from the collinear factorization using the nuclear PDF (EPS09; orange band) is also shown as well as other CGC-based results.

At intermediate rapidity $\eta = 2$, where the relevant x_2 becomes smaller, we show the results with the k_T factorized form (5) and the hybrid formula (6). It is remarkable that the hybrid formula at LO gives $R_{\mathrm{p}+Pb}$ systematically below the one from k_T factorization. However, exploratory inclusion of the partial NLO corrections tends to systematically increase the ratio (dash-dotted line) [5].

At the forward rapidity $\eta = 4$, where $x_2 \ll x_1 \lesssim 1$, we use the hybrid formalula. The nuclear modification factor $R_{\mathrm{p}+A}$ calculated with LO formula becomes significantly below unity over a wider range of p_T, while the one from the collinear factorization using nulclear PDF lies closer to unity.

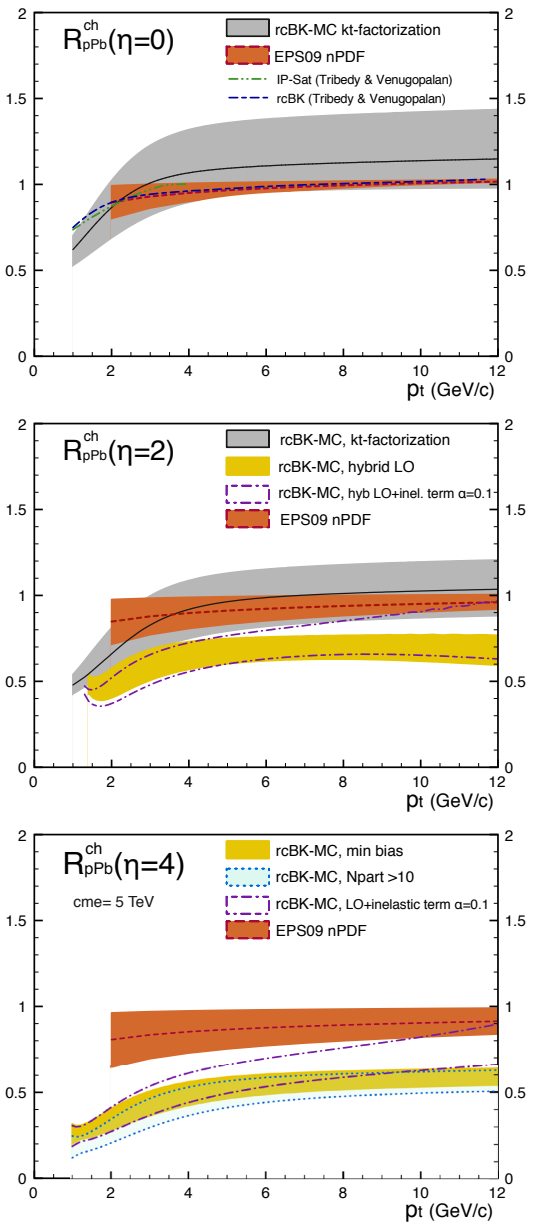

Figure 3. The nuclear modification factor $R_{\mathrm{p}+A}$ for single inclusive charged hadrons in minimum-bias p+Pb collisions at 5 TeV collision energy at rapidities 0, 2 and 4. The grey bands at η=0 and 2 correspond to the rcBK-MC results using k_T-factorization, eq. (5). In turn, the yellow bands at $\eta = 2$ and 4 have been obtained using the LO hybrid formalism, eq. (6), in minimum bias collisions. The blue band between the dotted lines also correspond to LO hybrid results for collisions with a centrality cut $N_{\mathrm{part}} > 10$. The dashed dotted curves at $\eta = 2$ and 4 correspond to the result including exploratory estimate for NLO contribution.

3.3 Limiting fragmentation

It will be worthwhile to touch upon here the topic of limiting fragmentation in high-energy hadron collisions [12]. The hypothesis of limiting fragmentation states that the hadron multiplicity dN/dy measured from the beam rapidity, $y' = y - Y^{\mathrm{beam}}$, at very high energies has a universal profile. This phenomenon was discussed in the context of the parton saturation/CGC already some years ago in Refs. [13, 14].

Recalling the kinematics, $x_{1,2} = (p_T/m)\exp(\pm y - Y^{\mathrm{beam}})$, we see that the hypothesis means that hadron production will become independent of $x_2 \ll 1$ of the dense target at forward rapidities $y \sim Y^{\mathrm{beam}}$ in the high energy limit. Since in the forward rapidity region we have $Q_s^2(x_2) \gg Q_s^2(x_1) \sim \Lambda^2_{\mathrm{QCD}}$, we can make a rough estimate

of the gluon multiplicity in the k_T factorization formula as

$$\begin{aligned}\frac{dN_g}{dy} &\sim \int \frac{d^2p_T}{p_T^2}\int d^2k_T\ \alpha_S\varphi_{y_1}(k_T)\,\varphi_{y_2}(|p_T-k_T|)\\ &\sim \int \frac{d^2p_T}{p_T^2}\,\alpha_S\varphi_{y_2}(p_T)\ \int d^2k_T\ \varphi_{y_1}(k_T)\\ &\sim \text{const.}\int^{Q_s^2(x_2)} d^2k_T\ \varphi_{y_1}(k_T)\\ &\sim x_1 g(x_1, Q_2(x_2)),\end{aligned} \tag{8}$$

where we have exploited the fact that $k_T \sim \Lambda_{\rm QCD}$ can be ignored in $\varphi_{y_2}(|p_T - k_T|)$ since $\varphi_{y_2}(p_T)$ is peaked around $p_T \sim Q_s(x_2) \gg k_T$. and the fact that

$$\int \frac{d^2p_T}{p_T^2}\alpha_S\varphi_{y_2}(p_T) \sim \int d^2p_T\tilde{\mathcal{N}}_A(p_T) = \text{const.} \tag{9}$$

In the last line of eq. (8), there appears the collinear gluon distribution, $x_1 g(x_1, Q_s(x_2))$, with the factorization scale $Q_s(x_2)$, which satisfies the Bjorken scaling at moderate x_1, i.e., it is almost independent of the factorization scale $Q_s(x_2)$. Thus we have confirmed that the rapidity distribution of the hadron multiplicity in the very forward region is determined by PDF of the projectile at large x_1 only.

There are experimental data of hadron multiplicity in a wide range of rapidities measured by the PHOBOS collaboration at RHIC energies, and also by UA1 at SPS at $\sqrt{s}$ from 53 to 900 GeV. The limiting fragmentation was examined with these data in the CGC framework in [14], providing a simple interpretation for the phenomenon. Now the LHC extends the energy range, and analyses of the limiting fragmentaion hypothesis are ongoing with the new data, e.g., in [15]

3.4 Heavy quark production in p-A collisions

The charm quark production in high-energy hadron collisions become sensitive to the gluon saturation when the saturation scale $Q_s(x)$ becomes comparable to or larger than the charm quark mass, $Q_s(x) \gtrsim m_c$. Because the charm quark component is negligible in the wave function of the incident hadron and are produced only from the gluon fusion in initial hard interactions, their production is regarded as a sensitive probe for the gluon distribution in the incident hadrons.

In p-A collisions, $Q_s(x)$ on the nucleus side is enhanced by the nuclear thickness factor as mentioned earlier, while the proton behaves as a dilute system of the partons. Partons from the proton probe the dense target, especially in the forward production region. We studied the charm quark production in p-A collisions at the LHC in [16–19].

In the CGC framework, the heavy quark pair production cross-section at the leading order in α_s with the transverse momentum $p_{q\perp}$ ($p_{\bar{q}\perp}$) and rapidity y_q ($y_{\bar{q}}$) of the (anti-) quark in minimum bias events of a dilute-dense system (e.g., pA) is given in the large-N_c limit as [20]

$$\begin{aligned}&\frac{d\sigma_{q\bar{q}}}{d^2p_{q\perp}d^2p_{\bar{q}\perp}dy_q dy_{\bar{q}}} = \frac{\alpha_s^2}{16\pi^4 C_F}\\ &\times\int\frac{d^2k_{2\perp}d^2k_\perp}{(2\pi)^4}\frac{\Xi(\boldsymbol{k}_{1\perp},\boldsymbol{k}_{2\perp},\boldsymbol{k}_\perp)}{k_{1\perp}^2k_{2\perp}^2}\,\varphi_{{\rm p},x_1}(k_{1\perp})\,\phi_{A,x_2}^{q\bar{q},g}(\boldsymbol{k}_{2\perp},\boldsymbol{k}_\perp)\,,\end{aligned} \tag{10}$$

where $\boldsymbol{p}_{q\perp} + \boldsymbol{p}_{\bar{q}\perp} = \boldsymbol{k}_{1\perp} + \boldsymbol{k}_{2\perp}$, and $\varphi_{\rm p}$ and $\phi_A^{q\bar{q},g}$ are the unintegrated gluon distribution function of the proton and the three-point function of the nucleus, respectively. Ξ is the hard matrix element, whose explicit expression is found in e.g. [16].

In the forward rapidity region, where x_1 becomes large while x_2 is much smaller, we can use the hybrid formula [16]:

$$\begin{aligned}&\frac{d\sigma_{q\bar{q}}}{d^2p_{q\perp}d^2p_{\bar{q}\perp}dy_q dy_{\bar{q}}} = \frac{\alpha_s^2}{16\pi^2 C_F}\\ &\times\int\frac{d^2k_\perp}{(2\pi)^2}\frac{\Xi_{\rm coll}(\boldsymbol{k}_{2\perp},\boldsymbol{k}_\perp)}{k_{2\perp}^2}\,x_1 g(x_1,\mu)\,\phi_{A,x_2}^{q\bar{q},g}(\boldsymbol{k}_{2\perp},\boldsymbol{k}_\perp)\,,\end{aligned} \tag{11}$$

where $x_1 g(x_1, \mu)$ is the collinear gluon distribution function with μ being factorization scale. $\Xi_{\rm coll}$ is the hard matrix element in the collinear approximation (see [16]).

The multi-point function $\phi_{A,x_2}^{q\bar{q},g}(\boldsymbol{k}_{2\perp},\boldsymbol{k}_\perp)$ appears in the formula becuase each of the quark pairs from the gluon splitting experiences the multiple interactions at its fixed transverse position in the dense target. This breaks the k_T factorization in the quark production[21]. This function $\phi_{A,x_2}^{q\bar{q},g}(\boldsymbol{k}_{2\perp},\boldsymbol{k}_\perp)$ can be expressed as a product of the dipole amplitude $\mathcal{N}_A$ in the large-N_c limit. We use the numerical soluton of the rcBK equation to describe the dipole amplitude $\mathcal{N}_A$ in the large-N_c expression.

We evaluate J/ψ production cross-section from the quark production spectrum, eq. (10) or eq. (11), employing the color evaporation model, in which the quark pair with its invariant mass below the threshold is assumed to form the bound state with a fixed probability irrespective of their color state. In this calculation we set the initial saturation scale of Pb to $Q_{s0,A}^2 = 3Q_{s0,{\rm p}}^2$ at $x_0 = 0.01$.

In Fig. 4 we show the nuclear modification factor of J/ψ in p-Pb collisions at $\sqrt{s} = 5.02$ TeV in mid and forward rapidity regions. Two bands correspond to the results with the formulas, eq. (10) and eq. (11), respectively. They yield similar results in the ratio. The $R_{{\rm p}+A}$ lies below unity reflecting the stronger gluon saturation in the nuclear target than in the proton in our calculation. The suppression is more remarkable at low p_T and at forward rapidity. We see that the result is in reasonable agreement with the experimental data both at mid and forward rapidities.

We describe D meson production at large p_T as a fragmentation process of the charm quark, and convolute the single quark production spectrum with a fragmentation function, $D(z)$, with z the fraction of the quark momentum carried by the D meson. We use a simple analytic form for $D(z)$ but the result of $R_{{\rm p}+A}$ should not be much sensive to its details.

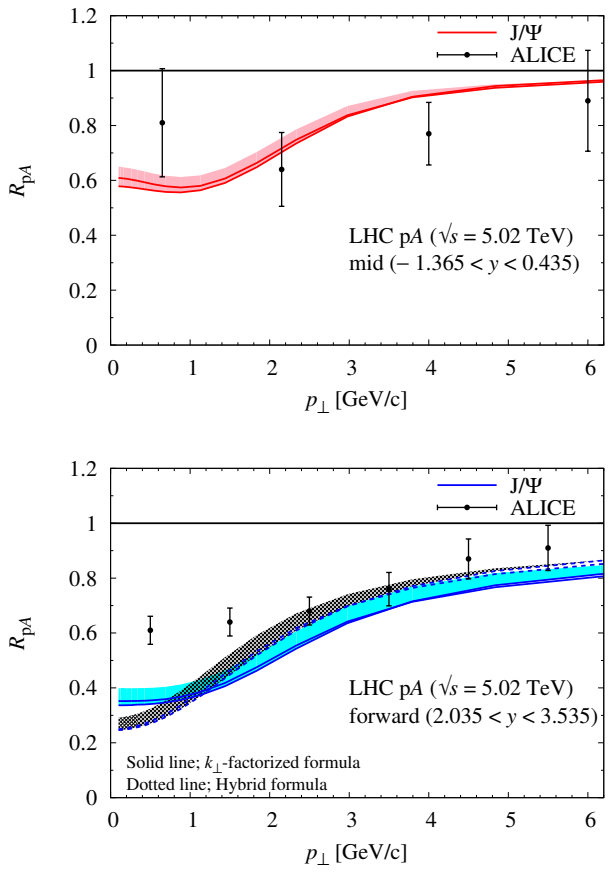

Figure 4. Nuclear modification factor of J/ψ production in p-Pb collisions at $\sqrt{s}$ = 5.02 TeV. Solid (dashed) band is the result with eq. (10) (eq. (11)). LHC data at mid and forward rapidities are taken from Ref. [22].

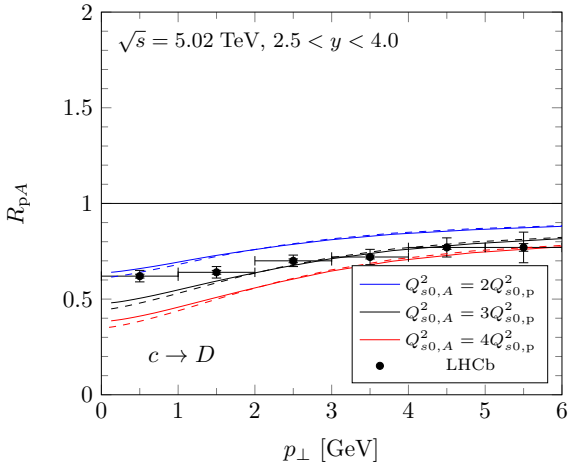

Figure 5. Nuclear modification factor of D meson production in p-Pb collisions at $\sqrt{s}$ = 5.02 TeV in the forward region. The initial saturation scale is varied as $Q^2_{s0,A} = (2,3,4)Q^2_{s0,p}$. Data is taken from Ref. [23].

In Fig. 5 we show R_{p+A} of D meson production in the forward rapidity region in p-Pb collisions at $\sqrt{s}$ = 5.02 TeV. On the nucleust side, we vary the initial saturation scale $Q^2_{s0,A}$ from 2 to 4 times the proton saturation scale $Q^2_{s0,p}$ at $x_0 = 0.01$, in order to check the sensitivity of our result to this parameter. We see that the D meson production is also sensitive the gluon saturation so that R_{p+A} is more suppressed as the initial saturation scale parameter $Q^2_{s0,A}$ is increased. Experimental data also shows a suppression in the p_T range shown here. The magnitude of the observed suppression is consistent with the result with $Q^2_{s0,A} = 3Q^2_{s0,p}$.

We also examined lepton production from D meosn decay in p-A collisions at $\sqrt{s}$ = 5.02 TeV in [18]. At mid rapidities the calculated ratio R_{p+A} is consistent with unity, but it shows significant suppression in the forward region.

4 Summary

We have recapped briefly the gluon saturation at small x in hadron wave function, which becomes relevant in high-energy hadron collisions and in the forward region. The CGC effective theory is the framework to treat this small-x component of the hadron wave function. We describe here the small-x gluons with the color dipole amplitude, $\mathcal{N}$, whose x-dependence is concisely governed by the rcBK evolution equation.

The CGC effective theory provides a theoretical framework to set up the initial condition for high-energy heavy-ion collisions, where the classical field approximation becomes more suitable for describing very early stage time evolution. The CGC initial condition inherits the longitudinal structure which is quite intriguing in the context of the observed phenomena such as the ridge structure of the observed two-particle correlation as well as the topological fluctuations.

We have studied the single particle spectrum produced in heavy ion collisions at the LHC, which gives a reasonable description of the data. We have also presented the interpretation of the limiting fragmentation which emerges naturally from gluon saturation phenomenon.

Charm quark production in high-energy hadron collisions is a sensitive probe to the gluon satuation. We have reported our numerical results for the nuclear modification factors of J/ψ and D meson in p-A collisions at the LHC, based on the CGC framework using the rcBK equation.

These analyses show that the CGC framework gives the semi-quantitative results uniformly in reasonable agreement with the data in high-energy hadron collisions. This implies that implementation of parton saturation effects is quite essential in modeling the hadron production at high-energy colliders and in cosmic ray events. One should notice that these numerical results employ the formula valid only at leading order in α_S. There are intensive efforts to extend the framework to the next-to-leading order accuracy and also to improve it by infra-red resummation.

Acknowledgements

This work was supported in part by Grants-in-Aid for Scientific Research, KAKENHI-16K05343.

References

[1] L. V. Gribov, E. M. Levin and M. G. Ryskin, Phys. Rept. **100**, 1 (1983)

[2] A. H. Mueller and J. w. Qiu, Nucl. Phys. B **268**, 427 (1986).

[3] For review, e.g., F. Gelis, E. Iancu, J. Jalilian-Marian and R. Venugopalan, Ann. Rev. Nucl. Part. Sci. **60**, 463 (2010)

[4] J. L. Albacete, N. Armesto, J. G. Milhano, P. Quiroga-Arias and C. A. Salgado, Eur. Phys. J. C **71**, 1705 (2011)

[5] J. L. Albacete, A. Dumitru, H. Fujii and Y. Nara, Nucl. Phys. A **897**, 1 (2013)

[6] I. Balitsky and G. A. Chirilli, Phys. Rev. D **88**, 111501 (2013)

[7] E. Iancu, A. H. Mueller and D. N. Triantafyllopoulos, JHEP **1612**, 041 (2016)

[8] K. Watanabe, B. W. Xiao, F. Yuan and D. Zaslavsky, Phys. Rev. D **92**, no. 3, 034026 (2015)

[9] A. Dumitru, F. Gelis, L. McLerran and R. Venugopalan, Nucl. Phys. A **810**, 91 (2008)

[10] J. P. Blaizot, F. Gelis and R. Venugopalan, Nucl. Phys. A **743**, 13 (2004)

[11] B. Abelev *et al.* [ALICE Collaboration], Phys. Rev. Lett. **110**, no. 3, 032301 (2013)

[12] J. Benecke, T.T. Chou, C.N. Yang and E. Yen, Phys. Rev. **188**, 2159 (1969)

[13] J. Jalilian-Marian, Phys. Rev. C **70**, 027902 (2004)

[14] F. Gelis, A. M. Stasto and R. Venugopalan, Eur. Phys. J. C **48**, 489 (2006); A. Stasto, Nucl. Phys. A **854**, 64 (2011)

[15] B. Kellers and G. Wolschin, arXiv:1901.06421 [hep-ph]

[16] H. Fujii and K. Watanabe, Nucl. Phys. A **915**, 1 (2013)

[17] H. Fujii and K. Watanabe, Nucl. Phys. A **920**, 78 (2013)

[18] H. Fujii and K. Watanabe, Nucl. Phys. A **951**, 45 (2016) Erratum: [Nucl. Phys. A **961**, 218 (2017)]

[19] H. Fujii and K. Watanabe, arXiv:1706.06728 [hep-ph]

[20] J. P. Blaizot, F. Gelis and R. Venugopalan, Nucl. Phys. A **743**, 57 (2004)

[21] H. Fujii, F. Gelis and R. Venugopalan, Phys. Rev. Lett. **95**, 162002 (2005)

[22] J. Adam *et al.* [ALICE Collaboration], JHEP **1506**, 055 (2015)

[23] R. Aaij *et al.* [LHCb Collaboration], JHEP **1710**, 090 (2017)